EUROPEAN TRANSACTIONS ON TELECOMMUNICATIONS
Eur. Trans. Telecomms. 2008; **19**:219–231
Published online 13 March 2007 in Wiley InterScience
(www.interscience.wiley.com) DOI: 10.1002/ett.1192

Information Theory

Minimum mean square error vector precoding

David A. Schmidt*, Michael Joham and Wolfgang Utschick

Associate Institute for Signal Processing, Technische Universität München, 80290 München, Germany

SUMMARY

We derive the *minimum mean square error* (MMSE) solution to vector precoding for frequency flat multiuser scenarios with a centralised multi-antenna transmitter. The receivers employ a modulo operation, giving the transmitter the additional degree of freedom to choose a *perturbation vector*. Similar to existing vector precoding techniques, the optimum perturbation vector is found with a closest point search in a lattice. The proposed MMSE vector precoder does not, however, search for the perturbation vector resulting in the lowest unscaled transmit power, as proposed in all previous contributions on vector precoding, but finds an optimum compromise between noise enhancement and residual interference. We present simulation results showing that the proposed technique outperforms existing vector precoders, as well as the MMSE *Tomlinson-Harashima precoder*, and compare the turbo-coded performance to the capacity of the broadcast channel. Copyright © 2007 John Wiley & Sons, Ltd.

1. INTRODUCTION

For the *broadcast channel* scenario [1] (i.e. *decentralised receivers*), the application of pure *precoding*, where the receivers only apply a simple scalar weighting, is necessary, since the joint optimisation of transmit and receive filters as in References [2–4] is impossible because the received signals cannot be transformed jointly by a non-diagonal matrix filter. *Linear precoding* (e.g. References [5–7]) is attractive due to its simplicity, because the data signal is linearly transformed at the transmitter and the received signal is only weighted with a scalar before quantisation.

However, we will focus on non-linear precoding in this paper due to the superior performance compared to linear precoders. One type of non-linear precoding is based on the minimisation of the *bit error probability* (BEP) as in References [8, 9]. Unfortunately, analytical solutions exist only for special channel matrices [9]; otherwise, the non-convex optimisation has to be solved numerically [8]. Thus, we do not consider BEP minimisation in this paper.

Instead, we focus on systems with *modulo receivers* (e.g. Reference [10]), where a modulo operator is applied to the weighted received signal prior to quantisation. If the modulation alphabet is a subset of the *fundamental Voronoi region* of the *lattice* $\mathbb{A}$ corresponding to the modulo operator, correctly estimated symbols are not affected by the modulo operator, since the modulo operator maps any element of the fundamental Voronoi region to itself (e.g. Reference [11]). Due to the property of the modulo operator that any element of a *coset* of the lattice $\mathbb{A}$ is mapped to the representative of the coset in the fundamental Voronoi region, the transmitter gains the degree of freedom to choose any element of the coset, whose representative is the data vector to be transmitted, as the desired value for the modulo operator input. This degree of freedom is employed by the scheme of Hochwald *et al.* [12], which is similar to *shaping without scrambling* for dispersive channels (cf. e.g. Reference [11]). Hochwald *et al.* proposed to use a linear transformation at the transmitter whose input is the desired element of the coset, that is the sum of the representative of the coset (data signal) and an element of the lattice $\mathbb{A}$ (*perturbation signal*). First, the linear transformation is chosen and kept fixed,

* Correspondence to: David A. Schmidt, Technische Universität München, Munich, Germany. E-mail: dschmidt@tum.de

Received 19 April 2006
Revised 4 December 2006
Accepted 19 December 2006

for example following a *zero-forcing* criterion resulting in the weighted channel pseudoinverse. In a second heuristic step, the perturbation signal is optimised to minimise the transmit power [12]. Since the lattice search necessary for finding the perturbation signal is closely related to the *sphere decoder* (e.g. Reference [13]), the algorithm was named *sphere encoder* [12]. However, we follow Reference [14] and simply call the scheme *vector precoding*. Note that the prominent *Tomlinson-Harashima precoding* (THP, see e.g. References [11, 15–21]), which is also based on modulo operators at the receivers, is a constrained type of vector precoding, since the elements of the perturbation vector are computed successively. We can therefore expect THP to be outperformed by vector precoding.

Motivated by the result that zero-forcing linear precoding is always outperformed by MMSE linear precoding (see References [6, 7]), Hochwald *et al*. also proposed a variant of vector precoding with a *regularised* pseudoinverse as the linear transformation at the transmitter in Reference [12]. Again, the perturbation signal was found by heuristically minimising the transmit power. As noted in Reference [12], the choice of the regularisation in the pseudoinverse is an open question and the results were obtained with a trial and error procedure. Thus, most publications on vector precoding concentrated on finding an appropriate linear transformation at the transmitter, but kept the heuristic of minimising the transmit power. In Reference [22], the linear *Wiener Filter* (WF) precoder was used as transformation at the transmitter and a similar scheme was applied to frequency selective MIMO systems in Reference [23]. In Reference [24], a *signal-to-interference-plus-noise-ratio* (SINR) criterion was used to find the linear transformation at the transmitter, but the power of some intermediate signal was minimised instead of the total transmit power.

To circumvent the computational complexity necessary for vector precoding, two suboptimum approaches have been proposed. In Reference [14], Windpassinger *et al*. simplified the closest point search in the lattice necessary for finding the perturbation signal with approximations by Babai [25], a technique known as *lattice reduction aided detector* at the receiver side [26]. Meurer *et al.* [27] proposed to split the symbols into groups to reduce the dimensionality of the problem for the closest point search.

Windpassinger [28] reported that the regularised vector precoder of Reference [12], which was considered to be the best vector precoder, is outperformed by MMSE-THP [21], even though THP computes the perturbation signal successively. This non-intuitive result can be explained by the heuristic of using two conflicting optimisations for the design of the linear transformation (minimisation of MSE or maximisation of SINR) and the perturbation signal (minimisation of the transmit power). Therefore, our aim is to find a single optimisation for vector precoding from which both, the linear transformation and the perturbation signal, result.

We will show how the well-known optimisations developed for linear precoding (e.g. Reference [7]) can be modified so that a design of the non-linear vector precoding based on a single optimisation is possible. Such a transformation will be performed for the optimisations of the popular *zero-forcing* linear precoding (e.g. References [5, 29–31]) and of the superior MMSE or *Wiener filter* (WF) linear precoding (e.g. References [7, 32, 33]). Neither do we consider *matched filter* precoding [34, 35] which is interference limited, nor linear precoding based on the SINR criterion (e.g. Reference [36]), because its application to non-linear precoding techniques still has open questions (see Reference [37]).

The resulting vector precoding optimisations allow any structure of the transmitter, that is we do not restrict ourselves to transmitters where the sum of the data signal and the perturbation signal is transformed by a linear filter as in Reference [12]. Nevertheless, as we will see, the optimum structure in the MMSE sense is of this form.

Our contributions are as follows.

1. We base vector precoding on *one optimisation*, instead of the state-of-the-art approach to employ two conflicting optimisations [12]. However, the single optimisation leads to a two-step procedure for vector precoding. First, the perturbation vectors are obtained by a nearest point search in a lattice. Second, the linear transformation is computed. Note that finding an optimisation for vector precoding is not only crucial for a deeper understanding but also for application, since the assumption of perfect *channel state information* (CSI) at the transmitter does not hold in reality. If the CSI is erroneous, a robust precoder design is necessary (as in e.g. Reference [38]), where a conditional mean has to be applied to the cost function of the optimisation for full CSI.
2. Motivated by the information theoretic results of Erez and Zamir in Reference [10] (see also Reference [39]), we use the *mean square error* (MSE) as the figure of merit to find a regularised vector precoder.
3. We derive MMSE vector precoding, that is we find a closed form solution for the necessary regularisation in the pseudoinverse. Interestingly, the structure of the linear transformation at the transmitter is independent of the choice for the perturbation vector.

4. We show that the state-of-the-art minimisation of the transmit power to obtain the perturbation vector is not optimum in the MMSE sense, that is for regularised vector precoding [12].
5. By including a zero-forcing constraint, we find that the scheme of Reference [12] without regularisation is the solution for zero-forcing vector precoding. Therefore, we show that the heuristically introduced rule for finding the perturbation vector by minimising the transmit power is optimal for zero-forcing vector precoding. Moreover, it is clear that our new MMSE vector precoding is superior to the variant in Reference [12], since MMSE vector precoding does not have to fulfill the zero-forcing constraint.
6. With simulations, we demonstrate that MMSE vector precoding outperforms all other vector precoding variants and in particular, is superior to MMSE-THP for any SNR contrary to the state-of-the-art vector precoders [12].

This paper is organised as follows: first, we review some concepts of optimised linear precoding, which will prove to be applicable to vector precoding as well. Then, in Section 3, we introduce the modulo operator at the receivers and show how the additional degree of freedom can be exploited by the precoder. In Section 4, we derive the MMSE vector precoder and finally compare its performance to that of existing schemes in Section 5.

1.1. Notation

Throughout the paper, we will denote vectors and matrices by lower and upper case bold letters, respectively. We use $\mathrm{E}[\bullet]$, $(\bullet)^*$, $(\bullet)^{\mathrm{T}}$, $(\bullet)^{\mathrm{H}}$, $\mathrm{tr}(\bullet)$, $\mathrm{Re}(\bullet)$ and $\mathrm{Im}(\bullet)$ for expectation, complex conjugation, transposition, conjugate transposition, the trace of a matrix, the real part and the imaginary part, respectively. $\lfloor\bullet\rfloor$ denotes the floor operator, which returns the largest integer that is smaller than or equal to the argument. The M-dimensional zero vector is $\mathbf{0}_M$ and the $N \times N$ identity matrix is $\mathbf{I}_N$. We use the same definition of derivatives of functions with complex arguments as in Reference [40]:

$$\frac{\partial f(z)}{\partial z} = \frac{1}{2}\left(\frac{\partial f(z)}{\partial \mathrm{Re}(z)} - \mathrm{j}\frac{\partial f(z)}{\partial \mathrm{Im}(z)}\right)$$

Furthermore, we define the derivative of a scalar function with respect to a vector or matrix to be a vector or matrix of the same dimensionality, containing the derivatives with respect to the elements of the vector or matrix.

2. LINEAR PRECODING

In the course of this paper, the concepts known from linear precoding techniques will turn out to also be applicable to vector precoding to a large extent. We therefore begin by reviewing the principle of linear precoding for frequency flat *multiple input multiple output* (MIMO) channels.

In our scenario, the transmitter employs N_{a} antennas, while the B decentralised receivers have a single antenna each. The transmitted symbols at the N_{a} antennas are collected in the vector

$$\boldsymbol{y}[n] = \left[y_1[n], \ldots, y_{N_{\mathrm{a}}}[n]\right]^{\mathrm{T}} \in \mathbb{C}^{N_{\mathrm{a}}}$$

and the received symbols of the B users are collected in the vector

$$\boldsymbol{x}[n] = \left[x_1[n], \ldots, x_B[n]\right]^{\mathrm{T}} \in \mathbb{C}^{B}$$

The frequency flat channel is represented by the matrix $\mathbf{H} \in \mathbb{C}^{B \times N_{\mathrm{a}}}$ containing the complex transmission coefficients from each of the transmit antennas to every receiver. Furthermore, the B receivers experience additive, stationary, zero-mean noise, collected in the vector $\boldsymbol{\eta}[n] \in \mathbb{C}^{B}$. We define the spatial noise covariance matrix as

$$\mathbf{R}_{\boldsymbol{\eta}} = \mathrm{E}\left[\boldsymbol{\eta}[n]\boldsymbol{\eta}^{\mathrm{H}}[n]\right] \in \mathbb{C}^{B \times B} \tag{1}$$

The received signal consequently evaluates to

$$\boldsymbol{x}[n] = \mathbf{H}\boldsymbol{y}[n] + \boldsymbol{\eta}[n] \in \mathbb{C}^{B} \tag{2}$$

In order to be able to transmit an independent stream of data symbols to each of the B users, the transmitter forms the transmit symbols $\boldsymbol{y}[n]$ by linearly combining the data symbols $s_1[n], \ldots, s_B[n]$:

$$\boldsymbol{y}[n] = \mathbf{P}\boldsymbol{s}[n] \in \mathbb{C}^{N_{\mathrm{a}}} \tag{3}$$

where $\mathbf{P} \in \mathbb{C}^{N_{\mathrm{a}} \times B}$ is the precoding matrix, the vector $\boldsymbol{s}[n] = [s_1[n], \ldots, s_B[n]]^{\mathrm{T}} \in \mathbb{A}^{B}$ with the covariance matrix

$$\mathbf{R}_{\boldsymbol{s}} = \mathrm{E}\left[\boldsymbol{s}[n]\boldsymbol{s}^{\mathrm{H}}[n]\right] \in \mathbb{C}^{B \times B}$$

contains the data symbols and $\mathbb{A}$ denotes the set of all points in the symbol constellation. In doing so, the transmitter must fulfill a transmit power constraint

$$\mathrm{E}\left[\|\boldsymbol{y}[n]\|_2^2\right] \leqslant E_{\mathrm{tr}} \tag{4}$$

The receivers apply a common gain control factor $g \in \mathbb{R}^{+}$, which can be acquired for example by means of training

DOI: 10.1002/ett

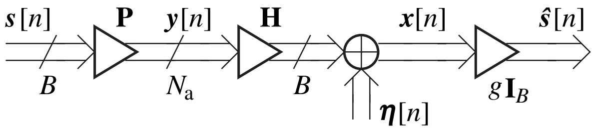

Figure 1. System model for linear precoding.

symbols, to the received signal. With Equations (2) and (3), the estimates of the data symbols at the receivers are

$$\hat{\boldsymbol{s}}[n] = g\mathbf{HP}\boldsymbol{s}[n] + g\boldsymbol{\eta}[n] \in \mathbb{C}^B \tag{5}$$

where the vector $\hat{\boldsymbol{s}}[n] = [\hat{s}_1[n], \ldots, \hat{s}_B[n]]^{\mathrm{T}} \in \mathbb{C}^B$ contains the estimates, which are finally passed on to the channel decoder. The system model for linear precoding is depicted in Figure 1.

The precoding matrix $\mathbf{P}$ can be designed according to different criteria. We begin with the most obvious approach, the inversion of the channel or *zero-forcing* (ZF) solution [5, 6, 29]. Here, we would like the cascade of precoder, channel and scaling by the receiver to be the identity matrix, thus allowing no interference between the users. If more than one solution is possible, we wish to further minimise the power of the amplified noise. This leads us to the optimisation problem

$$\{\mathbf{P}_{\text{linZF}}, g_{\text{linZF}}\} = \underset{\{\mathbf{P},g\}}{\arg\min}\, \mathrm{E}\left[\|g\boldsymbol{\eta}[n]\|_2^2\right]$$
$$\text{s.t.:}\quad g\mathbf{HP} = \mathbf{I}_B \quad \text{and} \quad \mathrm{E}\left[\|\mathbf{P}\boldsymbol{s}[n]\|_2^2\right] \leqslant E_{\text{tr}} \tag{6}$$

The solution to this problem is

$$\mathbf{P}_{\text{linZF}} = g_{\text{linZF}}^{-1}\mathbf{H}^{\mathrm{H}}\left(\mathbf{HH}^{\mathrm{H}}\right)^{-1} \tag{7}$$

where

$$g_{\text{linZF}} = \sqrt{\frac{1}{E_{\text{tr}}}\operatorname{tr}\left((\mathbf{HH}^{\mathrm{H}})^{-1}\mathbf{R}_s\right)}$$

so that the transmit power constraint is fulfilled with equality [7]. Due to the inversion of $\mathbf{HH}^{\mathrm{H}}$, it is necessary that $B \leqslant N_{\mathrm{a}}$ for the solution to exist.

Another approach is the minimisation of the *mean square error* (MSE) of the estimates at the receivers $\hat{\boldsymbol{s}}[n]$ with respect to the desired symbols $\boldsymbol{s}[n]$, the *minimum mean square error* (MMSE) or *Wiener filter* (WF) solution. Here, we do not specifically require the interference to be cancelled completely.

$$\{\mathbf{P}_{\text{linWF}}, g_{\text{linWF}}\} = \underset{\{\mathbf{P},g\}}{\arg\min}\, \mathrm{E}\left[\|\hat{\boldsymbol{s}}[n] - \boldsymbol{s}[n]\|_2^2\right]$$
$$\text{s.t.:}\quad \mathrm{E}\left[\|\mathbf{P}\boldsymbol{s}[n]\|_2^2\right] \leqslant E_{\text{tr}} \tag{8}$$

The solution (see References [7, 32, 41])

$$\mathbf{P}_{\text{linWF}} = g_{\text{linWF}}^{-1}\mathbf{H}^{\mathrm{H}}\left(\mathbf{HH}^{\mathrm{H}} + \xi\mathbf{I}_B\right)^{-1} \tag{9}$$

is somewhat similar to the ZF solution in Equation (7), the inverse, however, is regularised with an identity matrix weighted with the factor

$$\xi = \frac{\operatorname{tr}(\mathbf{R}_\eta)}{E_{\text{tr}}} \tag{10}$$

The scalar g_{linWF} is chosen to fulfill the power constraint with equality.

It is well researched and understood that the MMSE precoder always outperforms the ZF solution in terms of *bit error rate* (BER). An intuitive explanation is that the WF optimisation problem of Equation (8) becomes the ZF optimisation problem of Equation (6) if the additional constraint $g\mathbf{HP} = \mathbf{I}_B$ is introduced: when the constraint is plugged into Equation (5), the MSE simplifies to $\mathrm{E}[\|g\boldsymbol{\eta}[n]\|_2^2]$. Since the ZF problem is essentially the same as the WF problem with additional constraints that must be fulfilled, it becomes clear that less degrees of freedom are available for minimising the influence of the noise. While the WF precoder does not completely cancel interference between the users, it finds an optimum compromise between the noise gain and the residual interference. For a more in-depth discussion of linear precoders and the derivation of the solutions in Equations (7) and (9), the reader is referred to Reference [7].

3. PRECODING FOR MODULO RECEIVERS

We now introduce a simple non-linear operation at each of the receivers, which will later prove to enable great performance gains: the modulo operator M(•), defined as

$$\mathrm{M}(b) = b - \left\lfloor \frac{\mathrm{Re}(b)}{\tau} + \frac{1}{2} \right\rfloor \tau - \mathrm{j} \left\lfloor \frac{\mathrm{Im}(b)}{\tau} + \frac{1}{2} \right\rfloor \tau \ \in \mathbb{V}$$

DOI: 10.1002/ett

where the parameter τ is the *modulo constant* and

$$\mathbb{V} = \left\{ z \in \mathbb{C} \,\middle|\, -\frac{\tau}{2} \leqslant \mathrm{Re}(z) < \frac{\tau}{2},\ -\frac{\tau}{2} \leqslant \mathrm{Im}(z) < \frac{\tau}{2} \right\}$$

Put in words, the modulo operator maps both the real and the imaginary part of the operand to the interval $[-\tau/2, \tau/2)$, by adding integer multiples of τ and $\mathrm{j}\tau$. For example for $b = 2.2 - 3.1\mathrm{j}$ and $\tau = 4$, applying the modulo operation results in $\mathrm{M}(b) = -1.8 + 0.9\mathrm{j}$. In this case, the modulo operator added $-4 + 4\mathrm{j}$ to b.

We can equivalently think of $\mathrm{M}(\bullet)$ as an operation that maps any element of a *coset* of the *lattice* $\mathbb{A}$ to the representative of that coset in the *fundamental Voronoi region* $\mathbb{V}$ of the lattice $\mathbb{A}$, where $\mathbb{A} = \tau\mathbb{Z} + \mathrm{j}\tau\mathbb{Z}$ (e.g. Reference [11]).

We define the modulo operation applied to a vector $\boldsymbol{b} = [b_1, \ldots, b_K]^{\mathrm{T}} \in \mathbb{C}^K$ to be

$$\mathrm{M}(\boldsymbol{b}) = [\mathrm{M}(b_1), \ldots, \mathrm{M}(b_K)]^{\mathrm{T}} \in \mathbb{V}^K$$

that is the operator is applied elementwise. Again, the modulo operation applied to a vector can be thought of as mapping the element of a coset of the lattice $\mathbb{A}^K$ to the representative in the Voronoi region $\mathbb{V}^K$, where $\mathbb{A}^K = \tau\mathbb{Z}^K + \mathrm{j}\tau\mathbb{Z}^K$.

Now let us assume that each receiver applies this modulo operation after scaling the received signal. To ensure that correctly estimated symbols are not influenced by the modulo operator, we require $\mathbb{A} \subseteq \mathbb{V}$—that is the symbols must be elements of the fundamental Voronoi region $\mathbb{V}$—since $\mathrm{M}(b) = b$ for $b \in \mathbb{V}$. This requirement can be fulfilled by proper choice of the modulo constant τ. As a simple example scenario, we consider BPSK modulation and a real valued channel. The data symbol for a single receiver can be either $+1$ or -1; the modulo operation, however, also maps the values $+1 + \tau$, $+1 - \tau$, $+1 + 2\tau$, etc. to $+1$, as long as $\tau > 2$, to ensure $\{-1, +1\} \subseteq \mathbb{V}$. Therefore, if the transmitter would like to transmit the data symbol $+1$ to a certain user, it now has the additional option of transmitting $+1 + k\tau$ instead, where $k \in \mathbb{Z}$. This can also be thought of as a periodic extension of the symbol constellation [11]. When transmitting to B users, this means that the vector of data symbols for all users may be superimposed with any B-dimensional vector containing integer multiples of τ, henceforth referred to as the *perturbation vector* [12]. For complex valued transmission, the perturbation vector may be any lattice point of $\mathbb{A}^B$.

How can the transmitter benefit from this additional degree of freedom? One well-known precoding scheme in which the receivers employ the modulo operation is THP. The THP transmitter for a frequency flat MIMO channel (see e.g. References [18, 19, 21]) employs a successive interference cancellation procedure, in which the data streams are precoded one after another. In principle, the first symbol is transmitted unaltered; the second symbol is transmitted taking into account and subtracting the interference that will be caused by the first symbol, and so on, until the last symbol is transmitted with compensation for all other symbols. Every precoded symbol is also processed with the same modulo operator as is applied by the receivers. Thus, the amplitude of the transmit signal is strictly limited.

Similar to the linear precoders, THP can be designed according to the ZF criterion, in which no interference between users is allowed, or the MMSE (or WF) criterion, in which a compromise between interference and noise enhancement is found. Again, ZF-THP is clearly outperformed by WF-THP (see Section 5 and Reference [21]). The complexity of computing the feedforward and feedback filter for THP is cubic in the number of users, the precoding of the data symbols itself requires quadratic complexity [42].

Note that the choice of the perturbation vector in THP is a byproduct of the interference cancellation procedure: each time a precoded symbol passes the modulo operator, an integer multiple of both τ and $\mathrm{j}\tau$ is added to the respective component of the symbol vector; together, these extra summands constitute the perturbation vector. In contrast, we refer to precoding schemes that directly determine the perturbation vector as *vector precoding* schemes.

A very straightforward design for a vector precoder is shown in Figure 2 (cf. [12]). First, the vector of data symbols $\boldsymbol{s}[n]$ is superimposed with the perturbation vector $\boldsymbol{a}[n]$, then the resulting vector is processed by a linear precoding matrix $\mathbf{P}$. An obvious heuristic approach for the case $B \leqslant N_{\mathrm{a}}$ is to employ a linear ZF filter (cf. Equation 7) that removes all interference

$$\mathbf{P}_{\mathrm{VP}} = g_{\mathrm{VP}}^{-1}\mathbf{H}^{\mathrm{H}}\left(\mathbf{H}\mathbf{H}^{\mathrm{H}}\right)^{-1} \in \mathbb{C}^{N_{\mathrm{a}} \times B} \tag{11}$$

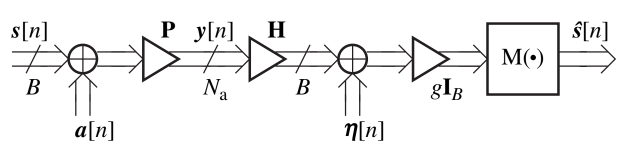

Figure 2. Heuristic vector precoder with perturbation and linear filter.

DOI: 10.1002/ett

and to find the perturbation vectors that minimise the unscaled transmit power

$$\boldsymbol{a}_{\mathrm{VP}}[n] = \underset{\boldsymbol{a}[n]\in\tau\mathbb{Z}^B+\mathrm{j}\tau\mathbb{Z}^B}{\arg\min} \left\| \mathbf{H}^{\mathrm{H}} \left(\mathbf{H}\mathbf{H}^{\mathrm{H}}\right)^{-1} (\boldsymbol{s}[n] + \boldsymbol{a}[n]) \right\|_2^2 \tag{12}$$

thus being able to fulfill a transmit power constraint as in Equation (4) with a maximised scaling factor g_{VP}^{-1} in Equation (11), resulting in minimised noise amplification at the receivers.

The discrete optimisation problem (12) is a closest point search in a lattice. The lattice consists of all vectors $\mathbf{H}^{\mathrm{H}}(\mathbf{H}\mathbf{H}^{\mathrm{H}})^{-1}\boldsymbol{a}[n]$, where $\boldsymbol{a}[n] \in \tau\mathbb{Z}^B + \mathrm{j}\tau\mathbb{Z}^B$. The matrix $\tau\mathbf{H}^{\mathrm{H}}(\mathbf{H}\mathbf{H}^{\mathrm{H}})^{-1}$ is called the *generator matrix* [13]. Of all points in this lattice, we are looking for the one with the lowest Euclidean distance to the point $-\mathbf{H}^{\mathrm{H}}(\mathbf{H}\mathbf{H}^{\mathrm{H}})^{-1}\boldsymbol{s}[n]$. The vector $\boldsymbol{a}[n]$ corresponding to that closest lattice point will then be the perturbation vector $\boldsymbol{a}_{\mathrm{VP}}[n]$. Closest point searches in lattices are a well-researched problem, the solution to which can be found with a number of algorithms, most notably the *Schnorr–Euchner* search strategy [43]. For a comprehensive overview, the reader is referred to Reference [13]. A very similar problem is the implementation of the *maximum likelihood* receiver for frequency flat MIMO channels as a *sphere decoder* (e.g. Reference [44]). The sphere decoder performs a search for the symbol constellation point closest to the received symbol vector. For QAM symbol constellations, the constellation points are points of a lattice, so the sphere decoder essentially performs a closest point search in a lattice. However, there is only a finite number of valid constellation points, consequently not all lattice points must be incorporated into the search. Nonetheless, the complexity of the sphere decoder grows exponentially with the number of users [45–47]. The lattice search problem at hand is even more complex than the sphere decoder, since all lattice points are possible solutions. In general, the complexity of a lattice search problem has been shown to be exponential in the number of users [13].

Determining the scaling factor g_{VP} for which a transmit power constraint as in Equation (4) is fulfilled is unfortunately not possible at filter design time, as the statistics of the perturbed symbols are unknown. We are forced to process blockwise, that is a block of data symbols must be precoded without scaling (e.g. by setting $g_{\mathrm{VP}} = 1$), then the transmit signal has to be scaled to fulfill the power constraint on average for the block before the signal is actually transmitted.

This vector precoder was proposed in Reference [12] and examined in References [14, 22]. In Section 4.3, we show that it is the zero-forcing solution to vector precoding. As can be seen in Section 5, it performs significantly better than ZF-THP.

The proposed precoder cancels interference between the different users completely. For both the linear filters and THP, it has been shown that allowing some interference can improve the performance significantly (e.g. References [7, 21]). As can be seen in Equation (9), this improvement is achieved by merely inserting a regularisation factor in the pseudo-inverse. By the same token, an improved vector precoder was also introduced in Reference [12], with the linear precoding matrix

$$\mathbf{P}_{\mathrm{regVP}} = g_{\mathrm{regVP}}^{-1}\mathbf{H}^{\mathrm{H}} \left(\mathbf{H}\mathbf{H}^{\mathrm{H}} + \zeta\mathbf{I}_B\right)^{-1} \in \mathbb{C}^{N_{\mathrm{a}}\times B} \tag{13}$$

The criterion for the choice of the perturbation vectors was also the minimisation of g_{regVP}:

$$\boldsymbol{a}_{\mathrm{regVP}}[n] = \underset{\boldsymbol{a}[n]\in\tau\mathbb{Z}^B+\mathrm{j}\tau\mathbb{Z}^B}{\arg\min} \left\| \mathbf{H}^{\mathrm{H}} \left(\mathbf{H}\mathbf{H}^{\mathrm{H}} + \zeta\mathbf{I}_B\right)^{-1} (\boldsymbol{s}[n] + \boldsymbol{a}[n]) \right\|_2^2 \tag{14}$$

The best regularisation factor ζ was however found by trial and error to be significantly lower than ξ in Equation (10) and also to be different depending on the number of users B (cf. [12]). Furthermore, simulation results show the performance of the regularised vector precoder to be worse than WF-THP for low to medium SNR (cf. Section 5).

4. OPTIMISED VECTOR PRECODING

In this section, we will introduce a framework for optimising the vector precoder according to different criteria. We derive the WF vector precoder, which is different from the above mentioned regularised technique (Equations 13 and 14) and show that the ZF vector precoder is identical to the interference cancelling vector precoder discussed in the previous section (Equations 11 and 12).

4.1. System model

In contrast to the previous sections, we do not impose a specific structure on the precoder (see Figure 3). We consider the transmission of one block of data symbols of length N_{B}, during which the scaling factor g is constant. We assume that the data symbols of the block $\boldsymbol{s}[1], \ldots, \boldsymbol{s}[N_{\mathrm{B}}]$

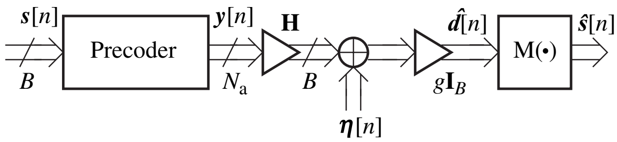

Figure 3. System model for vector precoding optimisation.

are known to the precoder. Based on the data symbols, the precoder chooses the transmit symbols $\boldsymbol{y}[1], \ldots, \boldsymbol{y}[N_\mathrm{B}]$. The scaled received symbols at the receivers

$$\hat{\boldsymbol{d}}[n] = g\mathbf{H}\boldsymbol{y}[n] + g\boldsymbol{\eta}[n] \in \mathbb{C}^B \tag{15}$$

are processed by the modulo operators, yielding the estimates

$$\hat{\boldsymbol{s}}[n] = \mathrm{M}\left(\hat{\boldsymbol{d}}[n]\right) \in \mathbb{V}^B$$

which are passed to the channel decoders. Again, the modulo constant τ must be large enough so that $\mathbb{A} \subseteq \mathbb{V}$.

Similar to the linear filters in Section 2, we impose a transmit power constraint. As the statistics of the transmit symbols are unknown, we average over the block instead of taking the expected value:

$$\frac{1}{N_\mathrm{B}} \sum_{n=1}^{N_\mathrm{B}} \|\boldsymbol{y}[n]\|_2^2 \leqslant E_\mathrm{tr} \tag{16}$$

The precoder has to perform two tasks:

1. It must choose the *virtual desired symbols*

$$\boldsymbol{d}[n] = \boldsymbol{s}[n] + \boldsymbol{a}[n] \in \mathbb{C}^B$$

for $n = 1, \ldots, N_\mathrm{B}$, where $\boldsymbol{a}[n] \in \tau\mathbb{Z}^B + \mathrm{j}\tau\mathbb{Z}^B$. In other words, it chooses which of the infinitely many vectors $\boldsymbol{d}[n]$ of the coset of $\mathbb{A}^B$ with the representative $\boldsymbol{s}[n] \in \mathbb{V}^B$ it will try to approximate. All members of this coset are mapped to $\boldsymbol{s}[n]$ by the receivers' modulo operators. We must keep in mind that the choice of the perturbation vector $\boldsymbol{a}[n]$ in general may have an influence on the MSE.
2. It must determine the transmit symbols $\boldsymbol{y}[n]$, for $n = 1, \ldots, N_\mathrm{B}$, so that the transmit power constraint of Equation (16) is fullfilled and the $\hat{\boldsymbol{d}}[n]$ approximate the $\boldsymbol{d}[n]$, for $n = 1, \ldots, N_\mathrm{B}$, according to some criterion. Inherent in the choice of the transmit symbols that fulfill the power constraint is the choice of the gain factor g.

4.2. Mean square error optimisation

First of all, we define the error to be the difference between the desired virtual symbol $\boldsymbol{d}[n]$ and the received symbol before the modulo operator $\hat{\boldsymbol{d}}[n]$. Clearly, when $\hat{\boldsymbol{d}}[n]$ is a good approximation of $\boldsymbol{d}[n]$, $\hat{\boldsymbol{s}}[n]$ will also be close to $\boldsymbol{s}[n]$. Incorporating the non-linear effect of the modulo operator into the cost function, on the other hand, would make the optimisation problem intractable. Note that we thereby follow along the lines of Peel *et al*. [12], where it is also the power of the scaled noise *before* the modulo operator that is minimised (cf. Equation 12).

We define the MSE for a given block of data symbols by averaging the symbol MSE over the whole block:

$$\varepsilon(\boldsymbol{a}[n], \boldsymbol{y}[n], g) = \frac{1}{N_\mathrm{B}} \sum_{n=1}^{N_\mathrm{B}} \mathrm{E}\left[\left\|\hat{\boldsymbol{d}}[n] - \boldsymbol{d}[n]\right\|_2^2 \,\middle|\, \boldsymbol{s}[n]\right]$$

Above MSE is conditioned on the symbols $\boldsymbol{s}[n]$ since these are known to the precoder. Consequently, the expected value is taken only over the noise. Note that conditioning on $\boldsymbol{s}[n]$ is crucial for the vector precoding optimisation, to preserve the known $\boldsymbol{s}[n]$ in the cost function. With Equations (15) and (1),

$$\begin{aligned}\varepsilon(\boldsymbol{a}[n], \boldsymbol{y}[n], g) &= \frac{1}{N_\mathrm{B}} \sum_{n=1}^{N_\mathrm{B}} \Big(\boldsymbol{d}^\mathrm{H}[n]\boldsymbol{d}[n] - 2g\mathrm{Re}\left(\boldsymbol{d}^\mathrm{H}[n]\mathbf{H}\boldsymbol{y}[n]\right) \\ &\quad + g^2\boldsymbol{y}^\mathrm{H}[n]\mathbf{H}^\mathrm{H}\mathbf{H}\boldsymbol{y}[n]\Big) + g^2\mathrm{tr}\left(\mathbf{R}_{\boldsymbol{\eta}}\right)\end{aligned} \tag{17}$$

We would like to find the *joint optimum* of all perturbation vectors $\boldsymbol{a}[n]$, all transmit vectors $\boldsymbol{y}[n]$ and the scaling factor g, constant for $n = 1, \ldots, N_\mathrm{B}$:

$$\{\boldsymbol{a}_\mathrm{WF}[n], \boldsymbol{y}_\mathrm{WF}[n], g_\mathrm{WF}\} = \underset{\{\boldsymbol{a}[n], \boldsymbol{y}[n], g\}}{\arg\min}\ \varepsilon(\boldsymbol{a}[n], \boldsymbol{y}[n], g)$$

$$\text{s.t.:} \quad \frac{1}{N_\mathrm{B}} \sum_{n=1}^{N_\mathrm{B}} \|\boldsymbol{y}[n]\|_2^2 \leqslant E_\mathrm{tr} \tag{18}$$

In this optimisation, the $\boldsymbol{y}[n]$ and g are continuous, while the $\boldsymbol{a}[n] \in \tau\mathbb{Z}^B + \mathrm{j}\tau\mathbb{Z}^B$ can only take certain discrete values. We therefore find the joint optimum in two steps: first, we assume that the $\boldsymbol{a}[n]$ are given and optimise over $\boldsymbol{y}[n]$ and g taking into account the transmit power constraint. To this end, we apply the method of Lagrangian multipliers, which yields necessary conditions for the optimal $\boldsymbol{y}[n]$ and g. It turns out that these conditions lead to a unique solution, which therefore is the global optimum for fixed $\boldsymbol{a}[n]$. Second, we further minimise the MSE by searching over the $\boldsymbol{a}[n]$ under the assumption that the optimum $\boldsymbol{y}[n]$ and g for the respective $\boldsymbol{a}[n]$ are employed. We would like to emphasise that even though we seem to be treating the continuous and discrete part of the optimisation separately, this procedure leads to the true optimum solution of Equation (18).

The Lagrangian function reads as

$$L(\boldsymbol{a}[n], \boldsymbol{y}[n], g, \lambda) = \varepsilon(\boldsymbol{a}[n], \boldsymbol{y}[n], g) + \lambda\left(\frac{1}{N_\mathrm{B}}\sum_{n=1}^{N_\mathrm{B}} \boldsymbol{y}^\mathrm{H}[n]\boldsymbol{y}[n] - E_\mathrm{tr}\right)$$

where $\lambda \in \mathbb{R}^{+,0}$. We set the derivatives with respect to $\boldsymbol{y}[n]$, $n = 1, \ldots, N_\mathrm{B}$, and g to zero, yielding the optimality conditions

$$\frac{\partial L(\ldots)}{\partial \boldsymbol{y}[n]} = \frac{1}{N_\mathrm{B}}\left(-g\mathbf{H}^\mathrm{T}\boldsymbol{d}^*[n] + g^2\mathbf{H}^\mathrm{T}\mathbf{H}^*\boldsymbol{y}^*[n] + \lambda\boldsymbol{y}^*[n]\right) = \mathbf{0}_{N_\mathrm{a}} \quad (19)$$

$$\frac{\partial L(\ldots)}{\partial g} = \frac{1}{N_\mathrm{B}}\sum_{n=1}^{N_\mathrm{B}}\Big(-2\mathrm{Re}\left(\boldsymbol{d}^\mathrm{H}[n]\mathbf{H}\boldsymbol{y}[n]\right) + 2g\boldsymbol{y}^\mathrm{H}[n]\mathbf{H}^\mathrm{H}\mathbf{H}\boldsymbol{y}[n]\Big) + 2g\,\mathrm{tr}\left(\mathbf{R}_{\boldsymbol{\eta}}\right) = 0 \quad (20)$$

A third condition for optimality is

$$\lambda\left(\frac{1}{N_\mathrm{B}}\sum_{n=1}^{N_\mathrm{B}} \boldsymbol{y}^\mathrm{H}[n]\boldsymbol{y}[n] - E_\mathrm{tr}\right) = 0 \quad (21)$$

Taking the transpose of Equation (19) and multiplying it from the right with $\boldsymbol{y}[n]N_\mathrm{B}/g$ yields

$$-\boldsymbol{d}^\mathrm{H}[n]\mathbf{H}\boldsymbol{y}[n] + g\boldsymbol{y}^\mathrm{H}[n]\mathbf{H}^\mathrm{H}\mathbf{H}\boldsymbol{y}[n] + \frac{\lambda}{g}\boldsymbol{y}^\mathrm{H}[n]\boldsymbol{y}[n] = 0$$

from which we can infer that $\boldsymbol{d}^\mathrm{H}[n]\mathbf{H}\boldsymbol{y}[n]$ must be real valued. With Equation (20), we obtain

$$\lambda = g^2\frac{\mathrm{tr}\left(\mathbf{R}_{\boldsymbol{\eta}}\right)}{\frac{1}{N_\mathrm{B}}\sum_{n=1}^{N_\mathrm{B}} \boldsymbol{y}^\mathrm{H}[n]\boldsymbol{y}[n]}$$

Since $g \in \mathbb{R}^+$, it becomes clear that $\lambda > 0$, that is the transmit power constraint must be fulfilled with equality for Equation (21) to hold. Together with Equation (16),

$$\lambda = g^2\frac{\mathrm{tr}\left(\mathbf{R}_{\boldsymbol{\eta}}\right)}{E_\mathrm{tr}} = g^2\xi$$

using the same definition of ξ as in Equation (10). Now $\boldsymbol{y}_\mathrm{WF}[n]$ and g_WF follow immediately from Equation (19) and the transmit power constraint of Equation (16), which is to be fulfilled with equality:

$$\boldsymbol{y}_\mathrm{WF}[n] = g_\mathrm{WF}^{-1}\mathbf{H}^\mathrm{H}\left(\mathbf{H}\mathbf{H}^\mathrm{H} + \xi\mathbf{I}_B\right)^{-1}\boldsymbol{d}[n] \quad (22)$$

$$g_\mathrm{WF} = \sqrt{\frac{\sum_{n=1}^{N_\mathrm{B}} \boldsymbol{d}^\mathrm{H}[n]\mathbf{H}\mathbf{H}^\mathrm{H}\left(\mathbf{H}\mathbf{H}^\mathrm{H} + \xi\mathbf{I}_B\right)^{-2}\boldsymbol{d}[n]}{E_\mathrm{tr}N_\mathrm{B}}} \quad (23)$$

where we also applied the matrix inversion lemma† (e.g. Reference [48]). $\boldsymbol{y}_\mathrm{WF}[n]$ and g_WF are the unique solution to the optimality conditions Equations (19), (20) and (21), and therefore are globally optimal for fixed $\boldsymbol{a}[n]$.

Before proceeding with the remainder of the optimisation, we would like to point out an important aspect of this intermediate result: whatever the best virtual desired symbol vectors $\boldsymbol{d}[n] = \boldsymbol{s}[n] + \boldsymbol{a}[n]$ turn out to be, we can obtain the optimum transmit symbols by linearly filtering $\boldsymbol{d}[n]$. Furthermore, only the scalar weight g_WF depends on $\boldsymbol{d}[n]$, but not the structure of the linear filter. We can conclude that the intuitively introduced structure of the precoder in Figure 2 is valid for the optimisation in Equation (18).

We now assume that the optimum gain factor and transmit vectors are employed and plug Equations (10), (22) and (23) into the MSE (17). The expression so obtained finally simplifies to

$$\begin{aligned}
&\varepsilon(\boldsymbol{a}[n], \boldsymbol{y}_\mathrm{WF}[n], g_\mathrm{WF}) \\
&= \frac{1}{N_\mathrm{B}}\sum_{n=1}^{N_\mathrm{B}}\left(\boldsymbol{d}^\mathrm{H}[n]\boldsymbol{d}[n] - \boldsymbol{d}^\mathrm{H}[n]\mathbf{H}\mathbf{H}^\mathrm{H}\left(\mathbf{H}\mathbf{H}^\mathrm{H} + \xi\mathbf{I}_B\right)^{-1}\boldsymbol{d}[n]\right) \\
&= \frac{\xi}{N_\mathrm{B}}\sum_{n=1}^{N_\mathrm{B}} \boldsymbol{d}^\mathrm{H}[n]\left(\mathbf{H}\mathbf{H}^\mathrm{H} + \xi\mathbf{I}_B\right)^{-1}\boldsymbol{d}[n] \\
&= \frac{\xi}{N_\mathrm{B}}\sum_{n=1}^{N_\mathrm{B}} (\boldsymbol{s}[n] + \boldsymbol{a}[n])^\mathrm{H}\left(\mathbf{H}\mathbf{H}^\mathrm{H} + \xi\mathbf{I}_B\right)^{-1}(\boldsymbol{s}[n] + \boldsymbol{a}[n])
\end{aligned}$$

Note that above MSE expression, to be minimised by the choice of the perturbation vectors $\boldsymbol{a}[n]$, $n = 1, \ldots, N_\mathrm{B}$, is different from the cost function for regularised vector precoding in Equation (14), even for $\zeta = \xi$.

The complete MSE $\varepsilon(\boldsymbol{a}[n], \boldsymbol{y}_\mathrm{WF}[n], g_\mathrm{WF})$ can be minimised by considering each summand (i.e. each time

† More precisely, we used the relation $(\mathbf{A}^\mathrm{H}\mathbf{A} + \alpha\mathbf{I})^{-1}\mathbf{A}^\mathrm{H} = \mathbf{A}^\mathrm{H}(\mathbf{A}\mathbf{A}^\mathrm{H} + \alpha\mathbf{I})^{-1}$, which follows directly from the matrix inversion lemma.

index n) separately. With any matrix $\mathbf{L}$ that fulfills

$$\left(\mathbf{H}\mathbf{H}^{\mathrm{H}} + \xi \mathbf{I}_B\right)^{-1} = \mathbf{L}^{\mathrm{H}}\mathbf{L}$$

which can be obtained, for example via Cholesky factorisation, we can rewrite the problem as

$$\boldsymbol{a}_{\mathrm{WF}}[n] = \underset{\boldsymbol{a}[n]\in\tau\mathbb{Z}^B + \mathrm{j}\tau\mathbb{Z}^B}{\arg\min} \; \|\mathbf{L}\,(\boldsymbol{s}[n] + \boldsymbol{a}[n])\|_2^2$$

for $n = 1, \ldots, N_{\mathrm{B}}$.

Consequently, the optimum choice of $\boldsymbol{a}[n]$ is again the solution to a closest point search in a lattice. In this case, the lattice is generated by the matrix $\tau\mathbf{L}$ and we are looking for the integer vector that corresponds to the lattice point closest to $-\mathbf{L}\boldsymbol{s}[n]$. Note that contrary to the regularised vector precoder proposed in Reference [12] (cf. Equations 13 and 14), this is not necessarily the point resulting in the lowest unscaled transmit power. Instead, we construct a lattice in which the Euclidean distance between a lattice point and the point $-\mathbf{L}\boldsymbol{s}[n]$ is a measure for the mean square error resulting from the choice of the perturbation vector corresponding to that lattice point.

We can summarise the MMSE or WF vector precoder as follows: for every symbol $\boldsymbol{s}[n]$ in the block, with $n = 1, \ldots, N_{\mathrm{B}}$, we determine the perturbation vector $\boldsymbol{a}_{\mathrm{WF}}[n]$ through a lattice search and filter the resulting virtual desired symbol $\boldsymbol{d}[n] = \boldsymbol{s}[n] + \boldsymbol{a}_{\mathrm{WF}}[n]$ with the regularised pseudo-inverse of the channel $\mathbf{H}^{\mathrm{H}}(\mathbf{H}\mathbf{H}^{\mathrm{H}} + \xi\mathbf{I}_B)^{-1}$. Finally, the whole block is scaled so that the transmit power constraint is fulfilled. The procedure is given in detail in Table 1.

4.3. Zero-forcing optimisation

Now we use the same method to derive the zero-forcing vector precoder. We only need to include complete interference cancellation as an additional constraint in the optimisation, which now reads as

$$\{\boldsymbol{a}_{\mathrm{ZF}}[n], \boldsymbol{y}_{\mathrm{ZF}}[n], g_{\mathrm{ZF}}\} = \underset{\{\boldsymbol{a}[n], \boldsymbol{y}[n], g\}}{\arg\min} \; \varepsilon\,(\boldsymbol{a}[n], \boldsymbol{y}[n], g)$$

$$\text{s.t.:} \quad \frac{1}{N_{\mathrm{B}}} \sum_{n=1}^{N_{\mathrm{B}}} \|\boldsymbol{y}[n]\|_2^2 \leqslant E_{\mathrm{tr}} \quad \text{and}$$

$$g\mathbf{H}\boldsymbol{y}[n] = \boldsymbol{d}[n], \quad n = 1, \ldots, N_{\mathrm{B}}$$

Due to the additional constraint, the MSE in Equation (17) simplifies to

$$\varepsilon\,(\boldsymbol{a}[n], \boldsymbol{y}[n], g) = g^2 \mathrm{tr}\left(\mathbf{R}_{\boldsymbol{\eta}}\right) \tag{24}$$

The solution for $\boldsymbol{y}_{\mathrm{ZF}}[n]$ and g_{ZF} can again be found with the method of Lagrangian multipliers and reads as

$$\boldsymbol{y}_{\mathrm{ZF}}[n] = g_{\mathrm{ZF}}^{-1}\mathbf{H}^{\mathrm{H}}\left(\mathbf{H}\mathbf{H}^{\mathrm{H}}\right)^{-1}\boldsymbol{d}[n]$$

$$g_{\mathrm{ZF}} = \sqrt{\frac{1}{E_{\mathrm{tr}} N_{\mathrm{B}}} \sum_{n=1}^{N_{\mathrm{B}}} \boldsymbol{d}^{\mathrm{H}}[n]\left(\mathbf{H}\mathbf{H}^{\mathrm{H}}\right)^{-1}\boldsymbol{d}[n]}$$

Plugging $\boldsymbol{y}_{\mathrm{ZF}}[n]$ and g_{ZF} into the MSE (24) yields

$$\varepsilon\,(\boldsymbol{a}[n], \boldsymbol{y}_{\mathrm{ZF}}[n], g_{\mathrm{ZF}}) = \frac{\xi}{N_{\mathrm{B}}} \sum_{n=1}^{N_{\mathrm{B}}} (\boldsymbol{s}[n] + \boldsymbol{a}[n])^{\mathrm{H}}\left(\mathbf{H}\mathbf{H}^{\mathrm{H}}\right)^{-1}(\boldsymbol{s}[n] + \boldsymbol{a}[n])$$

We can therefore find the optimum perturbation vectors with

$$\boldsymbol{a}_{\mathrm{ZF}}[n] = \underset{\boldsymbol{a}[n]\in\tau\mathbb{Z}^B + \mathrm{j}\tau\mathbb{Z}^B}{\arg\min} \left\|\mathbf{H}^{\mathrm{H}}\left(\mathbf{H}\mathbf{H}^{\mathrm{H}}\right)^{-1}(\boldsymbol{s}[n] + \boldsymbol{a}[n])\right\|_2^2$$

This is identical to the interference cancelling vector precoder proposed in Reference [12] (cf. Equations 11 and 12). Note that—contrary to the MMSE vector precoder—$B \leqslant N_{\mathrm{a}}$ is necessary for the existence of the zero-forcing vector precoder.

Table 1. The Wiener filter vector precoder.

factorize $(\mathbf{H}\mathbf{H}^{\mathrm{H}} + \xi\mathbf{I}_B)^{-1} = \mathbf{L}^{\mathrm{H}}\mathbf{L}$
for $n = 1, \ldots, N_{\mathrm{B}}$:
$\quad \boldsymbol{a}_{\mathrm{WF}}[n] \leftarrow \underset{\boldsymbol{a}[n]\in\tau\mathbb{Z}^B + \mathrm{j}\tau\mathbb{Z}^B}{\arg\min} \|\mathbf{L}(\boldsymbol{s}[n] + \boldsymbol{a}[n])\|_2^2$
$\quad \boldsymbol{y}[n] \leftarrow \mathbf{H}^{\mathrm{H}}(\mathbf{H}\mathbf{H}^{\mathrm{H}} + \xi\mathbf{I}_B)^{-1}(\boldsymbol{s}[n] + \boldsymbol{a}_{\mathrm{WF}}[n])$
$g_{\mathrm{WF}} \leftarrow \sqrt{\frac{1}{E_{\mathrm{tr}} N_{\mathrm{B}}} \sum_{n=1}^{N_{\mathrm{B}}} \boldsymbol{y}^{\mathrm{H}}[n]\boldsymbol{y}[n]}$
for $n = 1, \ldots, N_{\mathrm{B}}$:
$\quad \boldsymbol{y}_{\mathrm{WF}}[n] \leftarrow g_{\mathrm{WF}}^{-1}\boldsymbol{y}[n]$

5. SIMULATION RESULTS

For the simulation results presented in this section, we used a 16QAM symbol constellation and set the modulo constant τ to four times the distance between nearest neighbours in the symbol constellation. We generated the channel as a matrix with i. i. d. unit variance complex

DOI: 10.1002/ett

Gaussian distributed entries and assumed perfect channel state information at the transmitter. We compare WF vector precoding (WF-VP), ZF vector precoding (ZF-VP) and the heuristic regularised vector precoder (reg. VP) with the discussed linear precoding techniques (lin. WF and lin. ZF) and THP using the optimum precoding order [21] (WF-THP and ZF-THP). The regularised vector precoder was simulated with regularisation factor $\zeta = \xi$ (reg. VP) as well as with the regularisation factor found to be optimum in Reference [12], that is $\zeta = \xi/20$ (reg. VP $\xi/20$) for $B = N_a = 4$ users and transmit antennas and $\zeta = \xi/10$ (reg. VP $\xi/10$) for $B = N_a = 10$ (cf. Equations 10, 13, and 14). Since vector precoding techniques require blockwise processing to exactly fulfill a power constraint while THP and the linear precoders fulfill the power constraint on average, we scaled the transmit symbol blocks for THP and the linear precoders to exactly fulfill the power constraint as well, in order to ensure a fair comparison. We define E_S/N_0 as the ratio of the average transmit symbol energy per user to the noise power per user. Note that this ratio is equal to ξ^{-1} (10).

5.1. Uncoded simulations

For the uncoded *bit error rate* (BER) results in Figures 4 and 5, we assumed $B = N_a = 4$ users and transmit antennas, and $B = N_a = 10$ users and transmit antennas, respectively. We used blocklength $N_B = 100$ and averaged over 10 000 blocks transmitted over random channel realisations.

Clearly, the WF schemes always outperform the according ZF schemes, for linear precoding, THP, as well as vector precoding. In particular, the plots show that the WF vector precoder developed in this paper consistently outperforms all other schemes. Furthermore, as can be seen from the slope of the graphs for high SNR, only the vector precoding schemes have the potential to achieve full diversity order. The reason for this is that with THP, the data stream of the first user is precoded linearly, as the interference from the subsequent users is not yet known. For high SNR, the performance of the linearly precoded first user becomes dominant and the slope of the BER graph is the same as for the linear precoders.

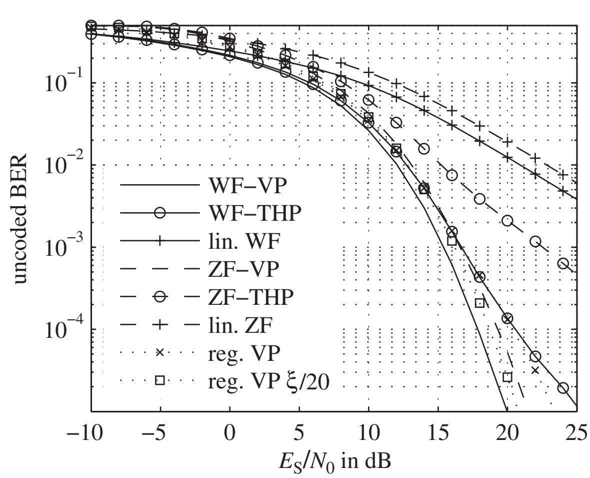

Figure 4. $B = 4$ users, $N_a = 4$ transmit antennas, 16QAM.

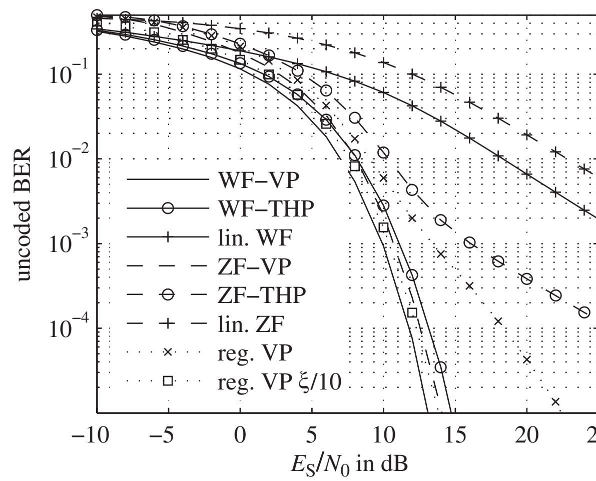

Figure 5. $B = 10$ users, $N_a = 10$ transmit antennas, 16QAM.

Even though the slope of the WF-THP graph does not decrease in the visible SNR range in Figure 5, it will behave similar to the WF-THP graph in Figure 4 for very high SNR, once the linearly precoded first user becomes the limiting factor.

The effect of regularising the ZF vector precoder depends on the regularisation factor. While the use of the factor $\zeta = \xi$ degrades the performance for high SNR compared to ZF-VP in both scenarios, significantly lower regularisation factors can lead to a slight improvement. However, in the BER region relevant for coded transmission, that is around a BER of 10^{-1}, WF-THP is better than the state-of-the-art regularised vector precoders (reg. VP $\xi/10$, $\xi/20$), even though with THP the elements of the perturbation vector are computed successively. Note that the new WF vector precoder outperforms WF-THP also in this BER region.

5.2. Turbo-coded simulations

For the coded BER results in Figures 6 and 7, we followed the simulation setup in Reference [12] and employed a standardisation parallel concatenated rate 1/3 code, with the feedforward polynomial $1 + D + D^3$ and the feedback

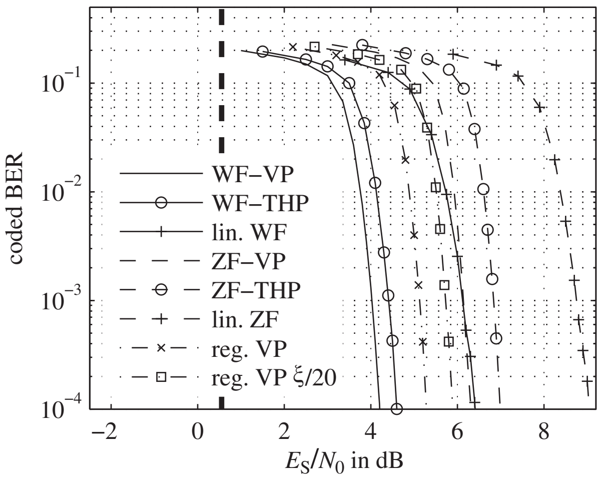

Figure 6. $B = 4$ users, $N_a = 4$ transmit antennas, 16QAM, code rate 1/2, dashed vertical line: ergodic broadcast channel capacity.

polynomial $1 + D^2 + D^3$ [49]. In order to achieve code rate 1/2, we punctured the non-systematic bits. We encoded blocks of 2000 data bits per user, resulting in 4000 coded bits or 1000 16QAM symbols per block. Each of these symbols was transmitted using an independent channel realisation (perfect interleaving), which was perfectly known to the transmitter, enabling a meaningful comparison with the *ergodic capacity of the broadcast channel*.

Furthermore, we determined the ergodic capacity of our i. i. d. channel model over E_S/N_0 by averaging over the capacity of 10 000 channel realisations, calculated with the

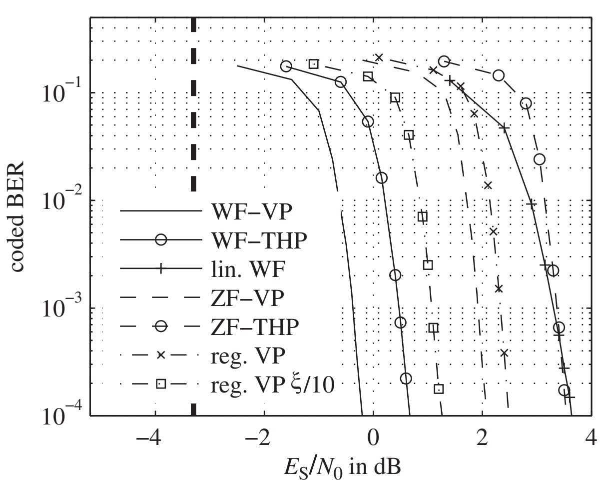

Figure 7. $B = 10$ users, $N_a = 10$ transmit antennas, 16QAM, code rate 1/2, dashed vertical line: ergodic broadcast channel capacity.

iterative waterfilling algorithm presented in Reference [50]. For reliably transmitting eight bits per channel use over the 4×4 channel, the minimum E_S/N_0 turned out to be approximately 0.5 dB, for transmitting 20 bits per channel use over the 10×10 channel, at least -3.3 dB are needed. These theoretical limits are represented in Figures 6 and 7 as dashed vertical lines.

With this setup, WF-VP is approximately 3.5 to 4 dB away from the ergodic capacity of the broadcast channel, where increasing the number of users apparently decreased the distance, a conclusion also reached in Reference [12]. The gain of WF-VP over WF-THP is relatively modest: approximately 0.5 dB for $B = N_a = 4$, and close to 1 dB for $B = N_a = 10$. In the scenarios at hand, WF-THP is clearly advantageous over the state-of-the-art regularised vector precoders from Reference [12].

6. CONCLUSION

We introduced a method for optimising the precoder for decentralised modulo receivers and derived the optimum precoder according to the MMSE criterion. Simulations show the MMSE vector precoder to perform slightly better than existing techniques, such as linear precoders, THP and regularised vector precoders. Also, by employing turbo codes, we were able to take a small step towards the information theoretic limit of the broadcast channel with a scheme based on separate channel coding of the data streams, even though all streams are given the same data rate. It appears that for higher dimensional systems, the distance to the information theoretic limit decreases. On the other hand, the complexity of the lattice search required for each precoded symbol quickly becomes prohibitive for real-time implementation.

Therefore, the results are more of theoretical interest by showing the performance gains achievable by introducing the simple modulo operator at the receivers. For practical implementation, successive precoders, such as THP or rounding-off procedures in a lattice with a reduced basis as in Reference [14], seem to be suited far better, as their complexity is quadratic, instead of exponential, per symbol vector, once the filters for the block have been computed.

REFERENCES

1. Cover TM, Thomas JA. *Elements of Information Theory*. John Wiley & Sons, Inc, New York, USA. 1991.

2. Salz J. Digital transmission over cross-coupled linear channels. *AT&T Technical Journal* 1985; **64**(6):1147–1159.
3. Yang J, Roy S. On joint transmitter and receiver optimization for multiple-input-multiple-output (MIMO) transmission systems. *IEEE Transactions on Communication* 1994; **42**(12):3221–3231.
4. Scaglione A, Stoica P, Barbarossa S, Giannakis GB, Sampath H. Optimal designs for space-time linear precoders and decoders. *IEEE Transactions on Signal Processing* 2002; **50**(5):1051–1064.
5. Vojčić BW, Jang WM. Transmitter precoding in synchronous multiuser communications. *IEEE Transactions on Communication* 1998; **46**(10):1346–1355.
6. Peel CB, Hochwald BM, Swindlehurst AL. A vector-perturbation technique for near-capacity multi-antenna multi-user communication—Part I: channel inversion and regularization. *IEEE Transactions on Communication* 2005; **53**(1):195–202.
7. Joham M, Utschick W, Nossek JA. Linear transmit processing in MIMO communications systems. *IEEE Transactions on Signal Processing* 2005; **53**(8):2700–2712.
8. Irmer R, Habendorf R, Rave W, Fettweis G. Nonlinear Multiuser Transmission using Multiple Antennas for TDD-CDMA. In *Proceedings of WPMC'03*, vol. 3, October 2003, pp. 251–255.
9. Weber T, Meurer M. Optimum Joint Transmission: Potentials and Dualities. In *Proceedings of WPMC'03*, vol. 1, October 2003, pp. 79–83.
10. Erez U, Zamir R. Achieving $\frac{1}{2}\log(1+\mathrm{SNR})$ on the AWGN channel with lattice encoding and decoding. *IEEE Transactions on Information Theory* 2004; **50**(10):2293–2314.
11. Fischer RFH. *Precoding and Signal Shaping for Digital Transmission*. John Wiley & Sons, Inc: New York, 2002.
12. Hochwald BM, Peel CB, Swindlehurst AL. A vector-perturbation technique for near-capacity multi-antenna multi-user communication—Part II: perturbation. *IEEE Transactions on Communication* 2005; **53**(3):537–544.
13. Agrell E, Eriksson T, Vardy A, Zeger K. Closest point search in lattices. *IEEE Transactions on Information Theory* 2002; **48**(8):2201–2214.
14. Windpassinger C, Fischer RFH, Huber JB. Lattice-reduction-aided broadcast precoding. *IEEE Transactions on Communication* 2004; **52**(12):2057–2060.
15. Tomlinson M. New automatic equaliser employing modulo arithmetic. *Electronic Letters* 1971; **7**(5/6):138–139.
16. Harashima H, Miyakawa H. Matched-transmission technique for channels with intersymbol interference. *IEEE Transactions on Communication* 1972; **20**(4):774–780.
17. Forney GD, Eyuboğlu MV. Combined equalization and coding using precoding. *IEEE Communications Magazine* 1991; **29**(12):25–34.
18. Ginis G, Cioffi JM. A Multi-user Precoding Scheme achieving Crosstalk Cancellation with Application to DSL Systems. In *Proceedings of Asilomar Conference on Signals, Systems, and Computers*, vol. 2, October 2000, pp. 1627–1632.
19. Fischer RFH, Windpassinger C, Lampe A, Huber JB. MIMO Precoding for Decentralized Receivers. In *Proceedings of ISIT 2002*, June/July 2002, p. 496.
20. Liu J, Duel-Hallen A. Tomlinson-Harashima Transmitter Precoding for Synchronous Multiuser Communications. In *Proceedings of CISS'03*, March 2003.
21. Joham M, Brehmer J, Utschick W. MMSE Approaches to Multiuser Spatio-Temporal Tomlinson-Harashima Precoding. In *Proceedings of ITG SCC'04*, January 2004, pp. 387–394.
22. Shao X, Yuan J, Rapajic P. Precoder Design for MIMO Broadcast Channels. In *Proceedings of ICC 2005*, vol. 2, May 2005, pp. 788–794.
23. Habendorf R, Irmer R, Rave W, Fettweis G. Nonlinear Multiuser Precoding for Non-Connected Decision Regions. In *Proceedings of SPAWC 2005*, June 2005, pp. 535–539.
24. Shi S, Schubert M. Precoding and Power Loading for Multi-Antenna Broadcast Channels. In *Proceedings of 38th Annual Conference on Information Sciences and Systems (CISS)*, March 2004.
25. Babai L. On Lovász' lattice reduction and the nearest lattice point problem. *Combinatorica* 1986; **6**(1):1–13.
26. Yao H, Wornell GW. Lattice-Reduction-Aided Detectors for MIMO Communications Systems. In *Proceedings of Globecom'02*, vol. 1, November 2002, pp. 424–428.
27. Meurer M, Weber T, Qiu W. Transmit Nonlinear Zero Forcing: Energy Efficient Receiver Oriented Transmission in MIMO CDMA Mobile Radio Downlinks. In *Proceedings of ISSSTA 2004*, September 2004, pp. 260–269.
28. Windpassinger C. Detection and Precoding for Multiple Input Multiple Output Channels. Ph.D. dissertation, Universität Erlangen-Nürnberg, 2004, ISBN 3-8322-2916-7.
29. Brandt-Pearce M, Dharap A. Transmitter-based multiuser interference rejection for the down-link of a wireless CDMA system in a multipath environment. *IEEE Journal on Selected Areas of Communications* 2000; **18**(3): 407–417.
30. Meurer M, Baier PW, Weber T, Lu Y, Papathanassiou A. Joint transmission: advantageous downlink concept for CDMA mobile radio systems using time division duplexing. *Electronics Letters* 2000; **36**(10):900–901.
31. Noll Barreto A., Fettweis G. Joint signal precoding in the downlink of spread spectrum systems. *IEEE Transactions on Wireless Communication* 2003; **2**(3):511–518.
32. Karimi HR, Sandell M, Salz J. Comparison between transmitter and receiver array processing to achieve interference nulling and diversity. In *Proceedings of PIMRC'99*, vol. 3, September 1999, pp. 997–1001.
33. Choi L, Murch RD. Transmit-preprocessing techniques with simplified receivers for the downlink of MISO TDD-CDMA Systems. *IEEE Transactions on Vehicular Technology* 2004; **53**(2):285–295.
34. McIntosh RE, El-Khamy SE. Optimum pulse transmission through a plasma medium. *IEEE Transactions on Antennas Propagation* 1970; **AP-18**(5):666–671.
35. Esmailzadeh R, Nakagawa M. Pre-RAKE diversity combination for direct sequence spread spectrum mobile communications systems. *IEICE Transactions on Communications* 1993; **E76-B**(8):1008–1015.
36. Schubert M, Boche H. Solution of the multiuser downlink beamforming problem with individual SINR constraints. *IEEE Transactions on Vehicular Technology* 2004; **53**(1):18–28.
37. Schubert M, Boche H. User Ordering and Power Allocation for Optimal Multiantenna Precoding/Decoding. In *Proceedings of ITG WSA 2004*, March 2004, pp. 174–181.
38. Dietrich FA, Utschick W. Robust Tomlinson-Harashima Precoding. In *Proceedings of PIMRC'05*, September 2005.
39. Forney GD, Jr. On the role of MMSE estimation in approaching the information-theoretic limits of linear Gaussian channels: Shannon meets Wiener. In *Proceedings of 2003 Allerton Conference*, October 2003.
40. Haykin S. *Adaptive Filter Theory* (2nd edn). Prentice Hall, Upper Saddle River, New Jersey, USA, 1991.
41. Choi RL, Murch RD. Transmit MMSE Pre-Rake Pre-processing with Simplified Receivers for the Downlink of MISO TDD-CDMA Systems. In *Proceedings of Globecom 2002*, vol. 1, November 2002, pp. 429–433.
42. Kusume K, Joham M, Utschick W, Bauch G. Efficient Tomlinson-Harashima Precoding for Spatial Multiplexing on Flat MIMO Channel. In *Proceedings of ICC 2005*, vol. 3, May 2005, pp. 2021–2025.
43. Schnorr CP, Euchner M. Lattice Basis Reduction: Improved Practical Algorithms and Solving Subset Sum Problems. *Mathematical Programming* 1994; **66**:181–199.
44. Viterbo E, Boutros J. A universal lattice code decoder for fading channels. *IEEE Transactions on Information Theory* 1999; **45**(5):1639–1642.
45. Hassibi B, Vikalo H. On the sphere-decoding algorithm I. Expected complexity. *IEEE Transactions on Signal Processing* 2005; **53**(8):2806–2818.

46. Vikalo H, Hassibi B. On the sphere-decoding algorithm II. Generalizations, second-order statistics, and applications to communications. *IEEE Transactions on Signal Processing* 2005; **53**(8):2819–2834.
47. Jaldén J, Ottersten B. On the complexity of sphere decoding in digital communications. *IEEE Transactions on Signal Processing* 2005; **53**(4):1474–1484.
48. Scharf LL. *Statistical Signal Processing*. Addison-Wesley, New York, USA. 1991.
49. ETSI. Universal Mobile Telecommunications System (UMTS): Multiplexing and channel coding (FDD) (3GPP TS 25.212 version 6.4.0), March 2005.
50. Jindal N, Rhee W, Vishwanath S, Jafar SA, Goldsmith A. Sum power iterative water-filling for multi-antenna Gaussian broadcast channels. *IEEE Transactions on Information Theory* 2005; **51**(4):1570–1580.

AUTHORS' BIOGRAPHIES

David Schmidt was born in Saarbrücken, Germany, in 1981. He studied electrical engineering at the Technische Universität München (TUM), Germany, from 2000 until 2005 and, in the fall of 2003, at Clemson University, Clemson, SC. He received the Dipl.-Ing. degree (*summa cum laude*) in the summer of 2005 and is currently a Research Assistant at the Associate Institute for Signal Processing, TUM, where he is also working towards his doctorate degree. His research interests include linear and nonlinear precoding techniques, as well as iterative and distributed equalization.

Michael Joham was born in Kufstein, Austria, 1974. He received the Dipl.-Ing. and Dr.-Ing. degrees (both *summa cum laude*) in electrical engineering from the Technische Universität München (TUM), Germany, in 1999 and 2004, respectively. Dr. Joham was with the Institute of Circuit Theory and Signal Processing at the TUM from 1999 to 2004. Since 2004, he has been with the Associate Institute for Signal Processing at the TUM, where he is currently a senior researcher. In the summers of 1998 and 2000, he visited *Purdue University, IN*. His main research interests are estimation theory, reduced-rank processing, and precoding in mobile communications. Dr. Joham received the *VDE Preis* for his diploma thesis in 1999 and the *Texas-Instruments-Preis* for his dissertation in 2004.

Wolfgang Utschick completed several industrial education programs before he received the diploma and doctoral degrees both with honors in electrical engineering from the Technische Universität München (TUM), in 1993 and 1998. In this period he held a scholarship of the Bavarian Ministry of Education for exceptional students and a scholarship of the Siemens AG. In 1993 he became a part-time lecturer at a Technical School for Industrial Education. From 1998 to 2002 he was co-director of the Signal Processing Group at the Institute of Circuit Theory and Signal Processing at the TUM. Since 2000 he is instrumental in the 3rd Generation Partnership Project as an academic consultant in the field of multi-element antenna wireless communication systems. In October 2002 Dr. Utschick was appointed Professor at the TUM in the Department of EI where he is head of the Associate Institute for Signal Processing. Wolfgang Utschick is SM of the VDE/ITG and SM of the IEEE where he is currently instrumental as AE for T-CAS. His research interests are in signal processing, communications, and applied mathematics in information technology.

DOI: 10.1002/ett